Radiative processes on a quantum computer

Paulo F. Bedaque [1,*] Ratna Khadka [2,†] Gautam Rupak [2,‡] and Muhammad Yusf [2,§]
[1]*Department of Physics, University of Maryland, College Park, Maryland 20742, USA*
[2]*Department of Physics & Astronomy and* HPC^2 *Center for Computational Sciences, Mississippi State University, Mississippi State, Mississippi 39762, USA*

(Received 13 February 2024; accepted 3 December 2024; published 7 March 2025)

Radiative processes, where a photon/neutrino is emitted as a result of a collision or decay of a particle, play a central role in atomic, nuclear, and particle physics. Their rate is determined by certain off-diagonal matrix elements between different initial and final states. We propose a method to compute them using quantum computers. It relies on a single extra qubit that, in a certain sense, represents the photon/neutrino. The generic formula relating this matrix element to the amplitude and frequency of oscillations of the extra qubit is derived for the near-resonance case. We demonstrate the feasibility of the method by using it in actual quantum computations and simulations of simple systems.

DOI: 10.1103/PhysRevC.111.034604

I. INTRODUCTION

Inelastic reactions are central to several branches of physics. They are responsible, for instance, for the production of all chemical elements in the early Universe and inside stars. They are, however, particularly difficult to describe theoretically, much more challenging than, for example, the bound states participating in these collisions. This difficulty arises partly because the numerical methods used in realistic calculations of nuclear/atomic bound states rely on stochastic methods and these methods, in one way or the other, use the evolution in imaginary time to project onto the ground state of the system. Scattering, however, is an inherently real-time phenomenon. In addition, stochastic methods, when applied to many-fermion systems using imaginary time techniques frequently have a sign-problem that renders them ineffective. A technique that employs real-time would be able to bypass both of these problems.

The recent advances in quantum computing hardware offer exactly that possibility. This is reflected in the growing list of nuclear structure calculations that includes, e.g., Refs. [1–6]. A more extensive list of publications can be found in the review article by Ayral *et al.* [7]. However, reaction calculations have been rare [8,9], and mere hardware improvements are not enough. Algorithms to make reaction calculations feasible are required. In this paper we introduce a general method to calculate radiative processes, where there is a photon/neutrino in either the final or initial state.

A quantum computer calculation of either $a(b,\gamma)c$ and/or its inverse $c(\gamma,b)a$ process where a, b, c are nuclei and γ a photon, proceeds through several steps. Firstly, the fermionic protons and neutrons states in three dimensions have to be encoded on the quantum register efficiently (see, for instance, the algorithms [10–12]). Secondly, a realistic Hamiltonian has to be chosen and coded in terms of universal quantum gates (simple examples will be shown below and general methods are extensively studied in Refs. [13–15]). Thirdly, the initial state where the participating clusters are formed, needs to be created (for instance, by adiabatic evolution). These steps are common to the calculation of static properties. Here, we focus on particularities of radiative capture reactions. One might simulate these reactions by starting from a state where the initial nuclei are widely separated, evolving it according to a realistic interaction (including the coupling to the photon/neutrino), and measuring the result after the final nuclei are formed or separated again. This mimics Nature but requires extremely large volumes and evolution times. An alternative, valid for elastic reactions, is to relate the energy levels of the system in a small volume to the phase shifts using the so-called Lüscher formula [16], as is done in lattice QCD.

Our proposal starts from the Fermi's golden rule, attributed to Dirac's derivation in 1927 [17], for calculating transition rates between initial $|E_i\rangle$ and final $|E_f\rangle$ states of an Hamiltonian H_0 owing to a perturbation O_T. The rate is controlled by the off-diagonal matrix element $\langle E_f|O_T|E_i\rangle$, the only dynamically nontrivial element required in the calculation. Contrary to diagonal matrix elements, the off-diagonal transition matrix elements are not given by the expectation value of any measurement and it is not *a priori* clear how to measure them using a quantum computer.

Here, we propose a method to measure such matrix elements in a quantum computer, and consequently, to compute reaction rates for radiative processes. The basic idea is simple and directly inspired by what actually happens in Nature, but simplified so it becomes practically feasible. In Nature, the photon γ in the radiative

*Contact author: bedaque@umd.edu
†Contact author: rk973@msstate.edu
‡Contact author: grupak@ccs.msstate.edu
§Contact author: mf1478@msstate.edu

capture process $a(b,\gamma)c$ entangles with the large Hilbert space of the environment. The probability for the photon to return and initiate the breakup reaction $c(\gamma,b)a$ is insignificant. However, in a simulation on a quantum computer, done in a small box, the reaction will proceed forward and backward $a(b,\gamma)c \leftrightarrow c(\gamma,b)a$ and will lead to a Rabi oscillation between the initial and final states. The aspects of this oscillation are determined by the same transition matrix element that determines the capture/decay rate. This way, the small volume becomes a useful feature, not a hindrance, for the calculation. Other simplifications of the realistic process can also be used. The electromagnetic field has an infinite number of modes, each one with a particular energy. In nonrelativistic systems the photon wavelengths are much larger than the typical sizes of the systems being studied and, in the case of radiative capture or decay, only photons in a very narrow range of energies significantly contribute to the process. Finally, since we are interested in the emission/capture of one photon, there is no need to describe two or more photon states. Thus, the electromagnetic field can be substituted by a single qubit. Its energy can be tuned at will and, in practice, it will be chosen close to resonance so the signal we are after is enhanced. We then demonstrate our method in a simple application to E1 electromagnetic transitions involving a particle in a simple harmonic oscillator (SHO). We also consider an even simpler two-level system and use an actual quantum computer to calculate the transition rates between them caused by the coupling to a photon.

II. TRANSITION MATRIX ELEMENT MEASUREMENT

We propose a general strategy to use quantum computers for measuring a transition matrix element of the form $\langle E_f|O_T|E_i\rangle$, where $|E_i\rangle$, $|E_f\rangle$ are eigenstates of the Hamiltonian H (with energy eigenvalues E_i, E_f, respectively) and O_T is a generic operator. For that, we consider the time evolution given by the Hamiltonian

$$H_T = \mathbb{1}\otimes H + \frac{\omega}{2}(\mathbb{1}-Z)\otimes\mathbb{1} + c_0 X\otimes O_T, \qquad (1)$$

acting on the tensor-product space of an additional qubit and the qubits representing the physical system of interest with c_0, a potentially dimensionful coupling. X, Y, Z are the usual Pauli matrices, and coupling the photon with a Y gate to O_T would also work.

Intuitively, one can think of the extra qubit as representing one "photon" cavity mode that can be either empty ($|0\rangle$) or occupied ($|1\rangle$) but not multiply occupied as a real photon mode could be. The "photon" frequency ω can be tuned arbitrarily; it is important to have the freedom to chose ω near the resonance regime $\omega \approx E_f - E_i$, which is an important difference between our method and Ref. [8]. A photon transition $|0\rangle \leftrightarrow |1\rangle$ is always accompanied by a transition between eigenstates of H. The rate of these transitions is set by the coupling c_0 and the value of the matrix element $|\langle E_f|O_T|E_i\rangle|$. As mentioned above, contrary to the case of radiative decay in empty space, the coupling of the quantum system to a single mode leads to oscillations between $|E_i\rangle$ and $|E_f\rangle$ instead of a decay from $|E_i\rangle$ to $|E_f\rangle$. In this case, the frequency and amplitude of these oscillations can be simply related to the matrix element of interest. For that, observe that for "photon" energies ω near resonance ($\omega \approx E_f - E_i$) the contribution of other eigenstates of the Hamiltonian are suppressed and only two states are relevant: $|1\rangle\otimes|E_i\rangle$ and $|0\rangle\otimes|E_f\rangle$, as they are the only states with total energy near E_f. The time evolution of the system is approximately governed by the Hamiltonian (in the basis formed by $|0\rangle\otimes|E_f\rangle$ and $|1\rangle\otimes|E_i\rangle$),

$$H_T^{\text{eff}} = \begin{pmatrix} E_f & \omega_1/2 \\ \omega_1/2 & E_i+\omega \end{pmatrix}, \qquad (2)$$

with $\omega_1 = 2c_0\langle E_f|O_T|E_i\rangle$. Assuming the initial state to be $|1\rangle\otimes|E_i\rangle$, the probability of finding the system in state $|0\rangle\otimes|E_f\rangle$ at a later time t is given by

$$P(t) = \frac{\omega_1^2}{(\Delta E-\omega)^2+\omega_1^2}\sin^2\frac{\sqrt{(\Delta E-\omega)^2+\omega_1^2}\,t}{2}, \qquad (3)$$

with $\Delta E = E_f - E_i$. Both the frequency and amplitude of the oscillations depend on the desired matrix element. This suggests the following algorithm:

(1) Encode the system and add an extra "photon" qubit.
(2) Prepare the initial state as $|1\rangle\otimes|E_i\rangle$.
(3) Evolve the initial state for time t with e^{-iH_Tt}.
(4) Measure the photon qubit.

Repeating this process many times and for several values of t determines $P(t)$ and from it $\langle E_f|O_T|E_i\rangle$ can be determined. Notice that it is not necessary to know E_f *a priori* as it can be determined by the fit to Eq. (3). Also, the transition probability is sizable even for poorly tuned values of ω. The case where two or more final states are close enough to be of importance can be worked out in a similar manner without altering the basic idea. We will not discuss the preparation of the initial state and assume there is an oracle that creates it.

It should be noted that this method can also be used to create an excited state $|E_f\rangle$ starting from $|E_i\rangle$. The particular excited state reached can be chosen by selecting an operator O_T with the proper quantum numbers and adjusting ω appropriately. Further, in an actual calculation on quantum computing hardware, a larger coupling c_0 can be chosen to make the probability amplitude larger and the oscillation frequency longer, so that measurements can be made at small t before the signal deteriorates significantly. Notice the flexibility introduced by the tunable "photon energy" ω. By tuning ω near resonance, the Hamiltonian H_T^{eff} eigenstates $|0\rangle_x$, $|1\rangle_x$ are now quantized along the x axis instead of the original quantization direction along the z axis. Time evolution then efficiently mixes the $|1\rangle = (|0\rangle_x - |1\rangle_x)/\sqrt{2}$ and $|0\rangle = (|0\rangle_x + |1\rangle_x)/\sqrt{2}$ states, a mechanism similar to nuclear magnetic resonance.

Example 1: E1 electromagnetic transition. As an example of the method described in the previous section, let us consider a simple model of an E1 transition matrix element in an one-dimensional quantum system.

The physical photon field $\boldsymbol{A}(\boldsymbol{r})$ that induces E1 transition in three dimensions is included in nonrelativistic quantum mechanics through gauge invariance. The momentum operator is modified through minimal coupling $\boldsymbol{P} \to \boldsymbol{P} + q\boldsymbol{eA}$ in

the kinetic energy term of the Hamiltonian $\boldsymbol{P}^2/(2m)$ of a free particle of mass m and charge qe. The E1 dipole operator is the term with a single $\boldsymbol{A}(\boldsymbol{r})$ field, $qe\boldsymbol{A}(\boldsymbol{r})\cdot\boldsymbol{P}/m$. One uses the commutator relation $[\boldsymbol{R}, H_0] = i\boldsymbol{P}/m$ between initial and final states, E_i and E_f for example, that are eigenfunctions of H to replace $qe\boldsymbol{A}(\boldsymbol{r})\cdot\boldsymbol{P}/m \to iqe(E_f - E_i)\boldsymbol{A}(\boldsymbol{r})\cdot\boldsymbol{R}$. In the large wavelength limit, $\boldsymbol{A}(\boldsymbol{r})$ can be taken to be $\boldsymbol{r}$ independent and the relevant transition matrix element for the E1 transition is then $\langle E_f|\boldsymbol{R}|E_i\rangle$.

Motivated by this physical picture, in one dimension, we consider the transition operator $O_T = X$ with a coupling $c_0 = qe\sigma^2$ where we introduced a mass scale σ to associate with the constant long wavelength $\boldsymbol{A}$ and factor of $E_f - E_i$. Discretizing space by a lattice with L sites, we arrive at the Hamiltonian, in natural units $\hbar = 1 = c$,

$$\hat{H} = -\frac{1}{2\hat{m}}\sum_l [\hat{\psi}_l^\dagger\hat{\psi}_{l+1} + \hat{\psi}_{l+1}^\dagger\hat{\psi}_l - 2\hat{\psi}_l^\dagger\hat{\psi}_l] + \sum_l \hat{V}_l\hat{\psi}_l^\dagger\hat{\psi}_l + \frac{\omega}{2}(\mathbb{1} - Z) + qe\sigma^2 X\sum_l l\hat{\psi}_l^\dagger\hat{\psi}_l, \quad (4)$$

where the second quantized particle field ψ_l destroys one particle at site l and $\hat{V}_l$ is the (discretized version) of the external potential the particle is subjected to. All the physical parameters have been scaled by appropriate factors of the lattice spacing a to get a dimensionless quantity denoted by a hat. The term proportional to $c_0 = qe\sigma^2$ is included in order to calculate the matrix element $\langle E_f|O_T|E_i\rangle$.

For a SHO potential, we take $V_l = m\omega_0^2 l^2/2$. The quantum register is comprised of $L+1$ qubits with the photon in the highest qubit and the lower L qubits representing lattice sites $l = -(L-1)/2, -(L-1)/2+1, \ldots, (L-1)/2$ for odd L. An even potential results in energy eigenfunctions with definite parity. An lth qubit equal to $|1\rangle$ indicates a particle on site l.

The time evolution is implemented by the second-order Lee-Suzuki-Trotter approximation formula [18]. In particular, the particle hopping term K with the prefactor $1/\hat{m}$, the potential energy term V with single-particle on-site potential $\hat{V}_l$, the photon energy term K_ω with frequency ω, and the E1 transition term H_{E1} with coupling $qe\sigma^2$ in Eq. (4) are implemented for a small time step Δt by a second-order approximation

$$\begin{aligned} &e^{-i(K+V+K_\omega+H_{E1})\Delta t} \\ &\quad = e^{-iK\Delta t/2}e^{-iV\Delta t/2}e^{-iK_\omega\Delta t/2}e^{-iH_{E1}\Delta t} \\ &\qquad \times e^{-iK_\omega\Delta t/2}e^{-iV\Delta t/2}e^{-iK\Delta t/2} + \mathcal{O}[(\Delta t)^3], \end{aligned} \quad (5)$$

that is more accurate than the first-order approximation with an estimated error $\mathcal{O}[(\Delta t)^2]$. Longer time unitary evolutions are obtained from the products of small Δt evolutions.

The circuit implementing the hopping term connecting wave function in neighboring lattice site l and $l+1$ are as shown in Fig. 1 with $\gamma = -\Delta t/m$ for Trotter time step Δt. We use an open boundary condition for the hopping term. The diagonal term $\hat{\psi}_l^\dagger\hat{\psi}_l/\hat{m}$ in the kinetic energy adds only an overall phase and can be discarded.

The potential energy for the harmonic oscillator is implemented by a position-dependent single qubit gate $R_z(\theta_l)$ with $\theta_l = -\hat{m}\hat{\omega}_0^2 l^2\Delta\hat{t}/2$. Similarly, the photon energy term is implemented with $R_z(-\omega\Delta t)$ on the highest qubit up to an overall phase.

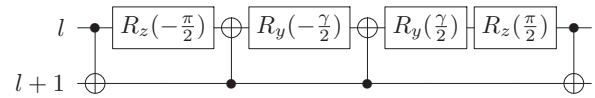

FIG. 1. Circuit for the hopping term. The lower qubits are on the upper wires.

The E1 transition described in Eq. (4) is implemented as in Fig. 2 with $\theta_l = qe\hat{\sigma}^2 l\Delta\hat{t}$.

To calculate the transition probability, we start with the exact ground state and a single photon. It is assumed that we have an oracle to generate the ground state. Then we evolve the system with the full Hamiltonian in Eq. (4). We use the second-order Lee-Suzuki-Trotter product formula for precision, and take measurements of the photon qubit. The transition probability is the probability of measuring a zero photon.

We simulated this circuit using the simulator Qulacs [19]. We used nuclear physics motivated values $m = 940\,\text{MeV}$, $\omega_0 = 8\,\text{MeV}$, $\sigma = 11\,\text{MeV}$ in the simulations. Lattice spacing a was varied between 0.5 fm–2 fm, keeping the physical volume fixed at $a(L-1) \sim 12\,\text{fm}$. We varied Δt to minimize Trotterization error to within 1%. The exact numerical ground state in a L-dimensional Hilbert space of a single particle in a SHO inside a box of size $a(L-1)$ was used for the initial state preparation.

In Fig. 3 we show simulation results for the SHO with $a = 0.6\,\text{fm}$, $L = 21$ and 5000 measurements. We refer to the simulation results as measurements, although they are actually calculations on a classical computer unlike the results from physical quantum processors that are obtained from actual measurements of probabilities. This is the standard convention in quantum computing literature. We compare the simulations with the analytical result for $P(t)$ from Eq. (3) with

$$\frac{1}{2}\omega_1^{(\text{th})} \equiv qe\sigma^2\int_{-\infty}^{\infty} dx\, x\phi_1^*(x)\phi_0(x) = \frac{qe\sigma^2}{\sqrt{2m\omega_0}}, \quad (6)$$

where $\phi_n(x)$ are the SHO eigenfunctions for the nth oscillator level. In Fig. 3(a) are shown results at $\omega = \omega_0/2$ and Fig. 3(b) are the results at resonance $\omega = \omega_0$ at $q = 1, 3$. Figure 3(c) compares the probability amplitudes at various ω and q values to the fit at $\omega = \omega_0/2$, see Table I.

In Table I we fit ΔE and ω_1 using Eq. (3) to the $P(t)$ data at photon frequency $\omega = \omega_0/2$ and resonance $\omega = \omega_0$, through a χ^2 minimization, for "charge" $q = 1, 2, \ldots, 5$. The fitted values for ΔE and ω_1 agree with the expected values ω_0 and $\omega_1^{(\text{th})}$, respectively. The finite volume and discretization errors seem negligible. Figures 3(a) and 3(b) show the fits at half

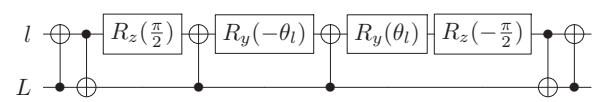

FIG. 2. Circuit for the E1 transition operator.

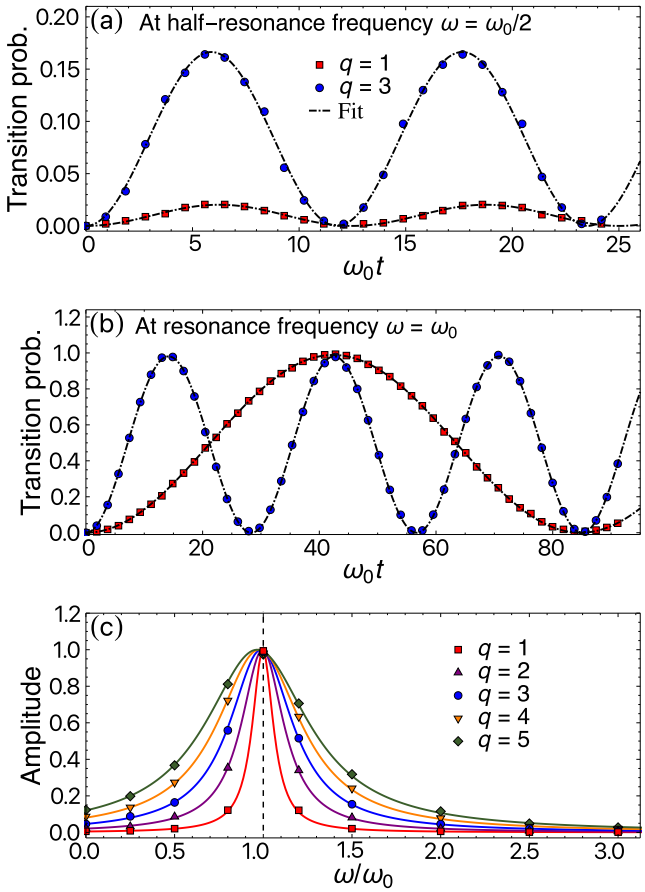

FIG. 3. SHO simulation results and fits to probability $P(t)$ in Eq. (3) as described in the text.

resonance $\omega = \omega_0/2$ and at resonance $\omega = \omega_0$, respectively, for only $q = 1, 3$.

Example 2: Two-level system. A proof-of-principle calculation of the algorithm on a physical quantum device is feasible. Consider a two-level system such as the one in Eq. (2). It can be thought of as the effective two-level Hamiltonian corresponding to the SHO simulated earlier or as the SHO states in an abstract linear vector space instead of coordinate space. However, this identification with SHO is not necessary. The system can be implemented with two qubits.

TABLE I. Fit parameters $\Delta\bar{E}$ and $\bar{\omega}_1$ for SHO are normalized to the expected oscillator frequency $\omega_0 = 8$ MeV and $\omega_1^{(\mathrm{th})}$, respectively. Thus, they are dimensionless. The first set of $(\Delta\bar{E}, \bar{\omega}_1)$ is from fits at $\omega = \omega_0/2$ and the second set with the superscript R is at resonance $\omega = \omega_0$. The fits for $q = 1, 3$ are shown in Figs. 3(a) and 3(b).

q	$\Delta\bar{E}$	$\bar{\omega}_1$	$\Delta\bar{E}^{(R)}$	$\bar{\omega}_1^{(R)}$
1	1.000(6)	0.936(2)	0.996(8)	0.9911(6)
2	0.994(5)	0.967(4)	0.988(11)	0.9866(10)
3	0.987(3)	0.972(3)	0.976(8)	0.9834(9)
4	0.977(2)	0.966(2)	0.961(10)	0.9793(13)
5	0.965(2)	0.958(2)	0.940(10)	0.9735(16)

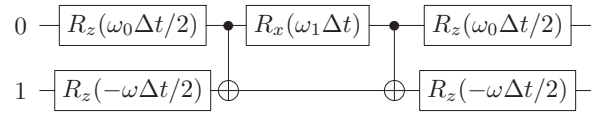

FIG. 4. Circuit for the two-level system.

In Eq. (1), we represent the two-level system by a single qubit with $H = \omega_0 Z/2$, and $O_T = X$ with SHO coupling $c_0 = qe\sigma^2/\sqrt{2m\omega_0} \equiv \omega_1/2$ (for notational convenience). The two-level Hamiltonian can be any transition operator not necessarily coupled to an external photon. A higher qubit is added for the photon to get $H_T = \frac{\omega_0}{2}\mathbb{1}\otimes Z + \frac{\omega}{2}(\mathbb{1} - Z)\otimes \mathbb{1} + \frac{\omega_1}{2} X\otimes X$.

The Δt evolution is implemented by the circuit in Fig. 4 using second-order Lee-Suzuki-Trotter approximation.

A noisy simulation using the qiskit simulator backend FakeManila [20] is presented in Fig. 5(a). A large value $q = 10$ was used in order to make the oscillations fast and therefore measurable before decoherence sets in. The rest of the parameter values for ω_0, σ, m, etc., were the same as the SHO. A time step $\Delta t = 1/\omega_0$ was small enough for this measurement. Measurements on the physical qubits 3 and 4 of ibmq_manila v1.0.35 (IBMQ-Manila) [21] are shown in Fig. 5(b). The ideal simulations, noisy simulations and hardware results in Fig. 5 were obtained from 1024 repeated measurements. We used a simple measurement error mitigation for the noisy simulations and hardware measurements where the corrected transition probability $P_c(t)$ is given by $P_c(t) = M^{-1}P_{\mathrm{measured}}$, where M is calculated from measurements on the initial states $|00\rangle$, $|01\rangle$, $|10\rangle$, and $|11\rangle$, see Ref. [22] and references therein. Error mitigation improves the signal noticeably for the noisy simulation but not for the hardware measurements. It would seem that even as the signal deteriorates, one can infer at resonance $\omega = \omega_0$, from

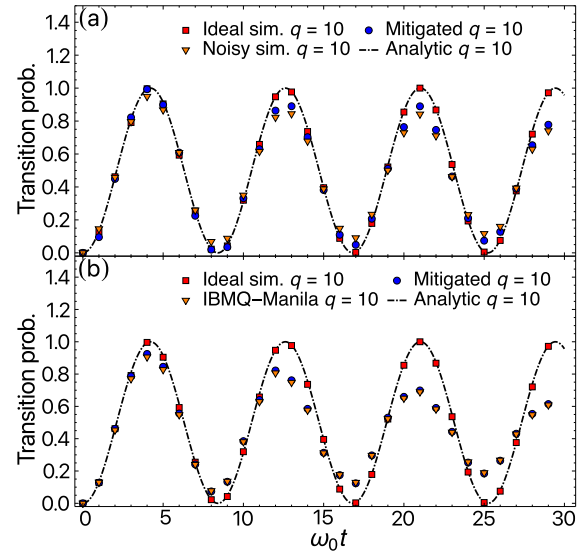

FIG. 5. Two-level results for ideal simulation, noisy simulation and IBMQ-Manila as described in the text.

the amplitude maxima $\omega_1^{(\text{meas.})} = (2n+1)\pi/t_{\max}$ or minima $\omega_1^{(\text{meas.})} = 2(n+1)\pi/t_{\min}$ for $n = 0, 1, \ldots$, in Fig. 5. Averaging over the maxima and minima locations, we find $\omega_1^{(\text{meas.})} \approx 1.03(3)\,\omega_1^{(\text{th})}$.

III. CONCLUSIONS

The exponential increase in the dimension of the Hilbert space with the number of particles, energy cutoffs, etc., poses a serious challenges to numerical calculations in nuclear physics and other fields where few/many-body physics is important. One possible path forward is the use of quantum computers, since they do not suffer from this problem as its Hilbert space also grows exponentially with the number of qubits. Among the many theoretical and practical issues facing this approach, we address the computation of off-diagonal matrix elements, essential for the study of inelastic processes. We develop an algorithm to achieve that with several advantages over previous attempts [8,9]. The same algorithm can be used to compute other off-diagonal matrix elements unrelated to inelastic scattering and to prepare, with high probability, excited states out of the ground state.

In the context of nuclear physics our method can be generalized to charge exchange reactions $a(b, c)d$ by introducing a resonance by coupling to a "photon" counting register. The algorithm works even if the desired transition operator O_T in Eq. (1) did not originally couple with an external photon or neutrino as demonstrated with the two-level result. In this paper, the Hamiltonian only had discrete levels unlike the continuum states in real processes such as $d(\gamma, n)p$. However, for calculations in a box, the continuum states are also discrete. A more general method involving the density of states $g(E)$ at continuum energy E near a resonance have to be explored in a future work.

ACKNOWLEDGMENTS

This work was supported in part by U.S. DOE Grants No. DE-SC0021195 (R.K., G.R., M.Y.), No. DE-SC0021143, No. DE-FG02-93ER40762, and No. DE-SC0021143 (P.F.B.) and NSF Grants No. PHY-1913620 (G.R., M.Y.), and No. PHY-2209184 (G.R.). The figures for this article have been created using SciDraw [23].

[1] E. F. Dumitrescu, A. J. McCaskey, G. Hagen, G. R. Jansen, T. D. Morris, T. Papenbrock, R. C. Pooser, D. J. Dean, and P. Lougovski, Phys. Rev. Lett. **120**, 210501 (2018).
[2] H.-H. Lu, N. Klco, J. M. Lukens, T. D. Morris, A. Bansal, A. Ekström, G. Hagen, T. Papenbrock, A. M. Weiner, M. J. Savage, and P. Lougovski, Phys. Rev. A **100**, 012320 (2019).
[3] M. J. Cervia, A. B. Balantekin, S. N. Coppersmith, C. W. Johnson, P. J. Love, C. Poole, K. Robbins, and M. Saffman, Phys. Rev. C **104**, 024305 (2021).
[4] O. Kiss, M. Grossi, P. Lougovski, F. Sanchez, S. Vallecorsa, and T. Papenbrock, Phys. Rev. C **106**, 034325 (2022).
[5] S. Sharma, T. Papenbrock, and L. Platter, Phys. Rev. C **109**, L061001 (2024).
[6] M. Yusf, L. Gan, C. Moffat, and G. Rupak, arXiv:2406.09231.
[7] T. Ayral, P. Besserve, D. Lacroix, and E. A. Ruiz Guzman, Eur. Phys. J. A **59**, 227 (2023).
[8] A. Roggero and J. Carlson, Phys. Rev. C **100**, 034610 (2019).
[9] A. Roggero, C. Gu, A. Baroni, and T. Papenbrock, Phys. Rev. C **102**, 064624 (2020).
[10] P. Jordan and E. Wigner, Z. Phys. **47**, 631 (1928).
[11] S. B. Bravyi and A. Y. Kitaev, Ann. Phys. **298**, 210 (2002).
[12] F. Verstraete and J. I. Cirac, J. Stat. Mech. (2005) P09012.
[13] E. van den Berg and K. Temme, Quantum **4**, 322 (2020).
[14] T. Tomesh, K. Gui, P. Gokhale, Y. Shi, F. T. Chong, M. Martonosi, and M. Suchara, in *Proceedings - 2021 International Conference on Rebooting Computing, ICRC* (IEEE, Piscataway, NJ, 2021), pp. 1-13.
[15] K. Gui, T. Tomesh, P. Gokhale, Y. Shi, F. T. Chong, M. Martonosi, and M. Suchara, arXiv:2001.05983.
[16] M. Lüscher, Nucl. Phys. B **354**, 531 (1991).
[17] P. A. M. Dirac, Proc. R. Soc. Lond. A **114**, 243 (1927).
[18] M. Suzuki, J. Math. Phys. **32**, 400 (1991).
[19] Y. Suzuki, Y. Kawase, Y. Masumura, Y. Hiraga, M. Nakadai, J. Chen, K. M. Nakanishi, K. Mitarai, R. Imai, S. Tamiya *et al.*, Quantum **5**, 559 (2021).
[20] M. S. Anis *et al.*, Qiskit: An open-source framework for quantum computing (2021).
[21] IBM Quantum, https://quantum-computing.ibm.com/ (2021), accessed: 2022-08-28.
[22] S. Bravyi, S. Sheldon, A. Kandala, D. C. Mckay, and J. M. Gambetta, Phys. Rev. A **103**, 042605 (2021).
[23] M. A. Caprio, Comput. Phys. Commun. **171**, 107 (2005).